

## Lithium Bond Chemistry in Lithium–Sulfur Batteries

Ting-Zheng Hou<sup>+</sup>, Wen-Tao Xu<sup>+</sup>, Xiang Chen<sup>+</sup>, Hong-Jie Peng, Jia-Qi Huang, and Qiang Zhang\*

**Abstract:** The lithium–sulfur (Li–S) battery is a promising high-energy-density storage system. The strong anchoring of intermediates is widely accepted to retard the shuttle of polysulfides in a working battery. However, the understanding of the intrinsic chemistry is still deficient. Inspired by the concept of hydrogen bond, herein we focus on the Li bond chemistry in Li–S batteries through sophisticated quantum chemical calculations, in combination with <sup>7</sup>Li nuclear magnetic resonance (NMR) spectroscopy. Identified as Li bond, the strong dipole–dipole interaction between Li polysulfides and Li–S cathode materials originates from the electron-rich donors (e.g., pyridinic nitrogen (pN)), and is enhanced by the inductive and conjugative effect of scaffold materials with  $\pi$ -electrons (e.g., graphene). The chemical shift of Li polysulfides in <sup>7</sup>Li NMR spectroscopy, being both theoretically predicted and experimentally verified, is suggested to serve as a quantitative descriptor of Li bond strength. These theoretical insights were further proved by actual electrochemical tests. This work highlights the importance of Li bond chemistry in Li–S cell and provides a deep comprehension, which is helpful to the cathode materials rational design and practical applications of Li–S batteries.

With the urgent demands for electric vehicles, smart grids, and electronic devices, an explosive growth of the capacity of energy storage units is strongly expected. The lithium–sulfur (Li–S) battery is quite promising and a breakthrough in routine lithium-ion battery research, and has been spotlighted in the entire energy storage field.<sup>[1,2]</sup> The Li–S battery has many remarkable advantages, that is, abundant resources, low costs, and high biocompatibility of cathode materials sulfur, as well as a high theoretical specific energy up to 2600 Wh kg<sup>−1</sup>.<sup>[3]</sup> However, there exists a lack of an elaborate landscape of the Li–S chemistry, thus radically impeding the practical applications.

One of the major problems in Li–S batteries is the so-called “shuttle” effect, which manifests as spontaneous dissolution and diffusion of soluble intermediates, Li poly-

sulfides, and a series of concurrent side reactions at interfaces or in solution. The shuttle effect not only gives rise to severe loss of active materials from the cathode, but also renders poor Coulombic efficiency and cycling life.<sup>[4]</sup> Conventional conductive materials, normally nanocarbon, can hardly mitigate the shuttle effect because of their intrinsic non-polarity in sharp contrast to attracting polar Li polysulfides. Physical confinement, either through porous scaffolds or external coating, is commonly adopted to retard the unbridled polysulfides, while it will take the expense of rate performance unless Li ion diffusivity within porous matrix or permeability through the coating shell is not compromised.<sup>[2,4,5]</sup> It is very challenging to simultaneously slow down the polysulfide diffusion and maintain rapid transport paths for Li ions.

Unlike physical confinement, surface chemistry initiated strategies are recently proposed by forming strongly coupled interfaces to interact with Li polysulfides.<sup>[6–8]</sup> The strong anchoring effect not only localizes polysulfides within the cathode scaffolds, but also facilitates preferable electrochemical contacts between polysulfides and conductive surfaces. Several theoretical studies have revealed the chemical nature of interactions between Li polysulfides and scaffolding materials.<sup>[7–11]</sup> Typically, binding energy, bond length, charge transfer, charge distribution, and density of state are analyzed to describe the chemical interactions. However, these analyses would rather be called qualitative, owing to the lack in effective linkage between these theoretical descriptors and experimental parameters. How to translate theoretical descriptors, obtained in vacuum, into experimentally available data, in actual environment with vast complexities in ions, solvents, electrical fields, etc., consequently raises a serious conundrum in reliability of interpretation.

Previously, Li bond theory has been introduced to interpret the strong binding between lithium polysulfides and hosts containing heteroatoms such as oxygen and nitrogen (N).<sup>[8,12]</sup> Particularly for pyridinic N (pN), the Li bond between Li and pN is theoretically regarded as a dipole–dipole interaction.<sup>[8]</sup> However, deeper understanding and better implementation of such a Li bond theory are in urgent demand for guiding rational experiments and materials innovation.

In this contribution, quantum chemical calculations, in combination with <sup>7</sup>Li nuclear magnetic resonance (NMR) spectroscopy, were employed to probe the Li bond chemistry in Li–S batteries. As indicated by natural bond orbital analysis, the strong dipole–dipole interaction not only originates from the electron-rich donor, but also is enhanced by the inductive and conjugative effect. A chemical upshift of Li polysulfides in <sup>7</sup>Li NMR spectra with the presence of an electron-donor is theoretically predicted and further verified

[\*] T.-Z. Hou,<sup>[†]</sup> W.-T. Xu,<sup>[†]</sup> X. Chen,<sup>[†]</sup> H.-J. Peng, Prof. J.-Q. Huang, Prof. Q. Zhang

Beijing Key Laboratory of Green Chemical Reaction Engineering and Technology, Department of Chemical Engineering  
Tsinghua University, Beijing 100084 (P.R. China)  
E-mail: zhang-qiang@mails.tsinghua.edu.cn

T.-Z. Hou,<sup>[†]</sup> W.-T. Xu<sup>[†]</sup>  
University of California Berkeley  
Berkeley, CA 94720 (USA)

[†] These authors contributed equally to this work.

Supporting information and the ORCID identification number(s) for the author(s) of this article can be found under:  
<https://doi.org/10.1002/anie.201704324>.

experimentally to validate the formation of Li bonds. The theoretically predicted strong binding can therefore be proved experimentally by using a single descriptor of chemical shift of Li polysulfides in  $^7\text{Li}$  NMR spectroscopy. Cathode hosts that enable large chemical upshift, that is, with strong Li bond, were probed to exhibit supreme electrochemical performance, suggesting that Li bond is of great importance and helpfulness to the rational design of cathodes, as well as other components such as anodes and electrolytes.

Being easily found in structural chemistry monographs, Li bond is an analogue of hydrogen (H) bond, which ubiquitously exists in nature to form dynamic networks and manage countless and transient molecular behaviors, for example, forming a double helix DNA (Figure 1 a). Such an ability is

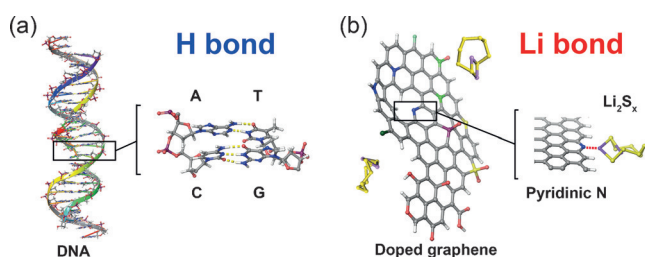


**Figure 1.** Schematic diagrams of a) H bond, in deoxyribonucleic acid (DNA), and b) Li bond, in Li-S batteries.

endowed by its weaker bonding nature than covalent or ionic bonds. Essentially, a hydrogen bond is formed between counterparts called “proton donors” and “proton acceptors”, respectively (e.g., in DNA, they are base pairs). Proton acceptors can be lone pairs,  $\pi$ -bonds, and polarizable electrons, covering a rather large number of elements and functional groups.

Li, as the closest congener of H, can also form a H bond analogue known as Li bond (Figure 1 b). Like H bond, Li bond is expected to offer a powerful perspective to understand the interfacial interactions in Li batteries, as long as the Li bond chemistry is unveiled unambiguously. The concept of Li bond can be traced back to 1959.<sup>[13]</sup> In Li bond theory, an electron-rich donor X interacts with a Li-Y cluster where Y is an anion. Because the stronger electropositivity of Li than H, the X...Li-Y interaction is stronger than the X...H-Y interactions. Nevertheless, a Li bond (X...Li) with properties somewhat similar to those of corresponding H bond (X...H) is found in X...Li-Y complexes. Furthermore, the pronounced tendency of Li compounds to form oligomers has long been known from colligative measurements, NMR investigations, and mass spectrometric observation.<sup>[14]</sup>

Since the pN provides one of the strongest binding to Li polysulfides ( $\text{Li}_2\text{S}_x$ ,  $x=4-8$ ) among all kinds of doped N species,<sup>[7,8]</sup> which is also advocated now, we take pN as a typical example to unveil the nature of Li bond herein. A B3LYP level theoretical analysis was performed. A model molecule, pyridine (PD), and a  $\text{Li}_2\text{S}_8$  cluster, as a representative of Li polysulfides, were used for exploring the Li bond chemistry. The optimized geometry in Figure 2 a shows a quite small distance between Li and N. As a comparison, the

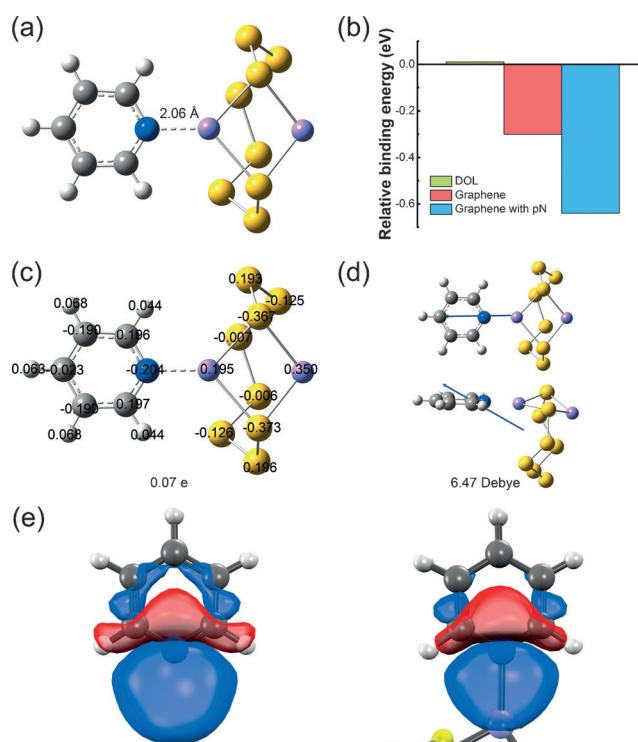


**Figure 2.** Li bond analysis in Li-S system. a) Optimized geometry of  $\text{Li}_2\text{S}_8$  binding to pyridine (PD), b) binding energies between  $\text{Li}_2\text{S}_8$  and DOL, graphene, or graphene doped with pyridinic nitrogen (pN), c) charge transfer between  $\text{Li}_2\text{S}_8$  and PD, d) dipole of  $\text{Li}_2\text{S}_8$ -PD cluster, and e) natural bond analysis of  $\text{Li}_2\text{S}_8$  before and after interacting with PD. Blue and red denote the positive and negative phase of the orbital, respectively. DOL: 1,3-dioxolane. Grey, blue, white, purple and yellow spheres are C, N, H, Li and S atoms, respectively.

calculated and measured Li-N bond lengths in  $\text{Li}_3\text{N}$  crystal are 2.09<sup>[8]</sup> and 2.06<sup>[15]</sup> Å, respectively, both quite close to the Li...N distance in  $\text{Li}_2\text{S}_8$ -PD cluster (2.06 Å). Due to the higher electronegativity of N (3.07) against Li (0.98), the formation of such a Li bond (Li...N) can be well explained by the Lewis acid-base theory.<sup>[14]</sup> The pN with an extra pair of electrons is considered as an electron-rich donor with filled p-orbitals that naturally acts as a Lewis base site and interacts with strong Lewis acid of terminal Li in lithium (poly)sulfides.<sup>[8]</sup> As a result, a relatively higher binding energy (−0.64 eV) of  $\text{Li}_2\text{S}_8$  is obtained for graphene with pN than pristine graphene and DOL solvent (Figure 2 b). What is more, the interaction energy of the Li bond (Li...pN) herein is also stronger than those of H bonds, which are typically in the range of 0.04–0.22 eV. As a consequence, Li bond, providing a strong interaction between Li and N (or other anchoring atoms), is propitious to form a strongly coupled interface for maintaining active substances and restricting the shuttle effect.

For other kinds of N dopants like pyrrolic N and graphitic N, it is true that they can also enhance the adsorption to polysulfides. However, pyrrolic N and graphitic N both form three  $\sigma$  bonds and one  $\pi$  bond in graphene lattice, offering no lone pair electrons to form Li bond. Therefore, the interactions of pyrrolic N and graphitic N are not identified as Li bonds, but normal intermolecular Keesom interactions.<sup>[7,8]</sup>

To further understand the nature of Li bond so as to understand its important role in Li–S chemistry, natural bond orbital analysis was employed to investigate charge transfer. Firstly, almost negligible negative charge transfer of  $0.07 e^-$  from PD to  $\text{Li}_2\text{S}_8$  is observed (Figure 2c), which is quite different from that in the ionic Li–N bond of  $\text{Li}_3\text{N}$  crystal. Despite the amount of charge transfer, the transfer directions of ionic bond (Li–N, Li to N) and Li bond (Li–pN) are poles apart. In case of Li bond, pN plays as the electron donor, while terminal Li in  $\text{Li}_2\text{S}_8$  plays as the acceptor. Hence, this Li bond interaction is differentiated from ionic interactions. Moreover, in contrast to the negligible charge transfer, the dipole is quite large as 6.47 Debye (Figure 2d), and formed concomitantly with the Li bond formation. Such an induced dipole in  $\text{Li}_2\text{S}_8$ -PD cluster is also much larger than those in  $\text{Li}_2\text{S}_8$  (2.87 Debye), PD (2.83 Debye), and their sum. Considering the large dipole with minor charge transfer, the nature of Li bond is probed as a dipole–dipole interaction instead of an typical “chemical” bond where charge transfer occurs.<sup>[8]</sup>

Besides dipole–dipole electrostatic interaction, there are additional conjugative and inductive effects in Li bond, as demonstrated by the natural bond analysis (Figure 2e).  $\pi$ -Electrons in the conjugated system of PD are obviously attracted to the Li–pN bond, similar to  $\pi$ -backdonation in metal–ligand complexes. The Li bond alters not only the electron density distribution of the aromatic ring, but also the bonding form of N. Concretely, the Wiberg bond order of N–C bond changes from 1.423 to 1.385 after PD binding to  $\text{Li}_2\text{S}_8$ . Simultaneously, the bond order of Li bond (Li–pN) is 0.108. Ultimately, the nature of Li bond as a dipole–dipole interaction is identified, and its bond strength mainly relies on the dipole along with extra conjugative and inductive effects.

The above theoretical calculation reveals the nature of Li bond in Li–S batteries. On top of that, however, the predicted bond strength has to be further correlated to certain experimental data. We still learn from the H bond theory: as proposed by Linus Pauling,<sup>[16]</sup> the H bond has a partial covalent bond nature, which had historically been in controversy until  $^1\text{H}$  NMR spectroscopy was employed to characterize H bonded nuclei.<sup>[17]</sup> By the same token,  $^7\text{Li}$  NMR spectroscopy should also be a powerful tool for characterizing Li bonds.

$^7\text{Li}$  NMR spectra of  $\text{Li}_2\text{S}_8$  before and after interacting with PD are collected both computationally and experimentally (Figure 3). Because the chemical shift is quite sensitive to the surrounding environment,  $^7\text{Li}$  NMR spectroscopy is superior in precisely probing possible Li bonds. During the calculation,

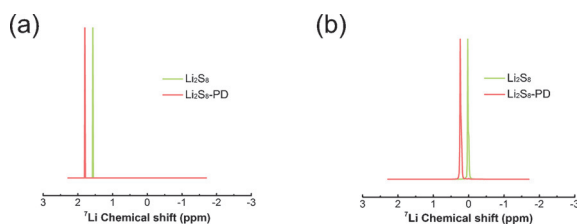


**Figure 3.** a) Theoretically calculated and b) experimentally obtained  $^7\text{Li}$  NMR spectra of  $\text{Li}_2\text{S}_8$  before and after interacting with PD.

solvation effects were treated with implicit Polarizable Continuum Model (PCM). Because the solvation exchange is not considered in this solvation model, there is a difference in the absolute values of the chemical shift between calculation (around 1.5 ppm) and experimental (around 0.0 ppm, in good accordance with literature<sup>[18]</sup>) results. However, variations of chemical shift are in good coincidence: the peak in NMR spectrum of  $\text{Li}_2\text{S}_8$  has an upshift of around 0.3 ppm with the presence of PD. The upshift to low field is ascribed to a deshielding effect on  $^7\text{Li}$  atom, which is similar to that in H bond theory. Such an upshift thus concurrently corresponds to the strong binding between Li and PD as calculated, also consistent with the case of  $\text{Li}_2\text{S}_8$ /pN-doped graphene in a recent report.<sup>[19]</sup> Therefore, the idea to correlate theoretically predicted Li bond strong interaction and experimental  $^7\text{Li}$  NMR data is realized in principle.

According to the above theoretical analysis and  $^7\text{Li}$  NMR experiments on  $\text{Li}_2\text{S}_8$ -PD model system, a series of insights can be subtracted: 1) pN has strong binding to  $\text{Li}_2\text{S}_8$  as suggested by the high binding energy; 2) a dipole–dipole interaction, namely Li bond, forms between  $\text{Li}_2\text{S}_8$  and pN to afford the strong binding but without remarkable charge transfer occurring; 3) the formation of Li–pN bond alters the local environment surrounding Li, resulting in an upshift in calculated NMR spectrum; 4) the theoretically predicted upshift, despite the difference of absolute values, exhibits the same trend as in experimental NMR spectra. These insights eventually make it, in principle, possible to use chemical shift in  $^7\text{Li}$  NMR spectroscopy to characterize the strength of Li bonds in actual electrode materials and working Li–S batteries, and to further interpret or anticipate the performance. Besides nitrogen, the possible interfacial properties of other dopant elements have been explored previously in silico<sup>[8]</sup> and it will be very interesting to study their interactions with polysulfides via NMR spectroscopy.

To fully validate that, thermally annealed graphene (G, annealed in Ar) and N-doped graphene (NG, annealed with  $\text{NH}_3$ ) were added in  $\text{Li}_2\text{S}_8$  solution (denoted as  $\text{Li}_2\text{S}_8$ -G and -NG, respectively), and their corresponding  $^7\text{Li}$  NMR spectra were collected subsequently (Figure 4a). The chemical shift of  $\text{Li}_2\text{S}_8$ -G is around 0.0 ppm, similar to that of pure  $\text{Li}_2\text{S}_8$  solution with the presence of solvents and co-salts.<sup>[18]</sup> The peak spread, with a half width from  $-0.29$  to  $0.60$  ppm, could be explained by the relatively weak interaction between Li ions and graphene. In contrast, the peak of the  $\text{Li}_2\text{S}_8$ -NG is much broader, with a half width from  $-0.76$  to  $3.57$  ppm, than that of  $\text{Li}_2\text{S}_8$ -G cluster, because many kinds of doped N species (e.g., pN, pyrrolic N, graphitic N, etc.) are induced to the carbon lattice at different topological sites (e.g., zigzag edge, armchair edge, kink, and defect), resulting in a large variety in the local environment surrounding Li.<sup>[10]</sup> Nevertheless, it is noticed that the broad peak is obviously asymmetric and there is a small but unignorable split. The right part is at the same position as in the NMR spectrum of  $\text{Li}_2\text{S}_8$ -G, corresponding to Li interacting with undoped carbon sites; while the left part exhibits an upshift to low field with mean position located at  $1.50$  ppm, suggesting the formation of Li bond with doped N species. Notably, the value of this upshift is greater than the value in the PD model experiment.



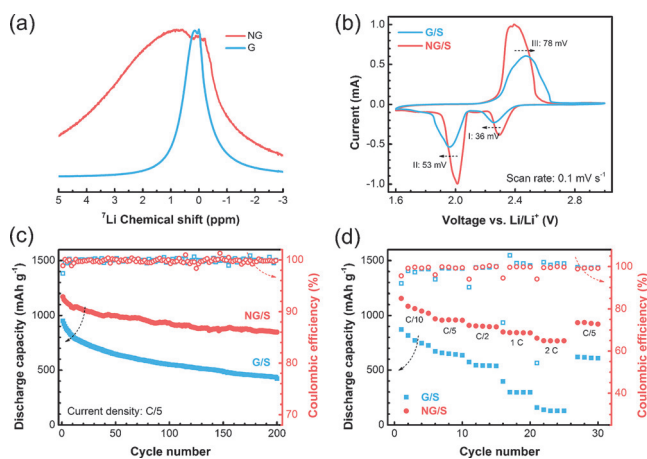


**Figure 4.** a) The  $^7\text{Li}$  NMR spectra of  $\text{Li}_2\text{S}_8$ -G and -NG; b) Cyclic voltammetric (CV) curves, c) cycling performance at a current density of 0.2 C ( $1.0\text{ C} = 1672\text{ mA g}^{-1}$ ), and d) rate performance of G and NG-based sulfur cathodes (denoted as G/S and NG/S, respectively).

The difference could be rationalized by the different chemical environments of N species and the stronger conjugative effect of graphene that could form stronger interactions.<sup>[8]</sup> Furthermore, the broadening of the peak can be also ascribed to the stronger binding of  $\text{Li}_2\text{S}_8$ -NG. According to NMR theory, slower molecular reorientation rate will reduce the  $T_2$  relaxation (Spin-Spin relaxation) time, causing stronger Heisenberg-Uncertainty-Principle broadening effect. Thus, the  $^7\text{Li}$  NMR spectrum is broadened due to stronger intermolecular confinement. Therefore, the chemical shift in  $^7\text{Li}$  NMR spectroscopy is a simple but quite promising descriptor that is able to quantify the interaction strength between Li polysulfides and host materials based on Li bonds.

To evaluate the functions of Li bond in working batteries, Li-S coin cells were further assembled using G and NG as the host materials, respectively. CV curves of both G/S and NG/S cathodes exhibit a typical Li-S electrochemistry in ether based electrolytes: two cathodic peaks appear at 2.2–2.4 V (peak I) and 1.9–2.1 V (peak II), accounting for successive reduction of sulfur to long-chain  $\text{Li}_2\text{S}_x$  ( $x = 4-8$ ), and further to insoluble  $\text{Li}_2\text{S}_2/\text{Li}_2\text{S}$ , respectively; while during the reverse scan, there is only one broad anodic peak at 2.3–2.7 V (peak III), probably due to the overlap of multiple current responses (Figure 4b). Despite the similar redox characteristics, NG/S enables significantly reduction in voltage polarization (36, 53, and 78 mV for peak I–III, respectively) in comparison with G/S. Concurrently, the CV peaks of NG/S are much sharper and more prominent than those of G/S. All of the above distinctions indicate that NG/S, with favorable Li bonds formed during electrochemical reactions, profoundly promotes the reaction kinetics. As indicated previously, both electrical conductivity and polysulfide/ $\text{Li}_2\text{S}$  affinity of host materials affect the reaction kinetics.<sup>[9,11]</sup> Herein the Li bond formation facilitates the intermolecular binding and charge transfer, accounting for the enhanced kinetics.

The enhancement in the reaction kinetics is also reflected through cycling and rate tests. At C/5 ( $1\text{ C} = 1672\text{ mA g}^{-1}$ ), G/S delivered an initial discharge capacity of  $951\text{ mAh g}^{-1}$ ; while the initial capacity of NG/S was  $1172\text{ mAh g}^{-1}$ , ca. 23 % higher

(Figure 4c). After 200 cycles, the difference was more profound: NG/S maintained a capacity of  $848\text{ mAh g}^{-1}$ , corresponding to a low cyclic decay rate of 0.14 %; on the contrary, only  $423\text{ mAh g}^{-1}$  was retained for G/S and the capacity decay was  $\approx 100\%$  faster. The Coulombic efficiency was generally above 99 % during cycling, and thus the different cycling performance is mainly attributed to the cathode side, that is, the formation of Li bonds. In addition to cycling stability at low rate, NG/S also exhibited a superior rate performance with capacities of 1156, 970, 909, 850, and  $793\text{ mAh g}^{-1}$  retained at C/10, C/5, C/2, 1 C, and 2 C, which were 32, 44, 58, 114, and 393 % higher than those of G/S, respectively (Figure 4d). The polarization of NG/S was also notably less severe than that of G/S at both low and high rates (see Figure S1 in the Supporting Information). Such a remarkable high rate capability of NG/S is in good accordance with CV curves and can be ascribed to the better affinity of NG to Li polysulfides and  $\text{Li}_2\text{S}$ , which facilitates mainly though Li bonds. Such strong interactions also contribute to the better cycling stability as it helps to anchor mobile intermediates, thereby mitigating the loss of active phases.

If one checks literatures, it would be easily found that the use of N and/or O doped carbon, as well as other polar substrates, like  $\text{TiC}$ ,<sup>[11]</sup> hydroxides,<sup>[20]</sup> and so on, have significantly enhanced the sulfur utilization. In fact, the interpretation to these results can also be sought in the view of as-proposed Li bond theory in this work. It is very likely that the Li bond interaction contributes the strong binding between polysulfides and polar substrates in these systems. A bold vision is proposed that high throughput screening of host materials based on this theory, theoretically or experimentally, could enable the rational design for boosting battery performance in the near future.

In summary, sophisticated quantum chemical calculations, in combination with  $^7\text{Li}$  NMR spectroscopy, was employed to probe the Li bond chemistry in Li-S batteries. Li polysulfides were found to form Li bond with an electron-rich donor. The Li bond is categorized as a kind of dipole–dipole interaction. Theoretically predicted and experimentally  $^7\text{Li}$  NMR spectra of Li polysulfides are in good accordance as chemical shifts move to low field with Li bond formation. Consequently, the chemical shift in  $^7\text{Li}$  NMR spectroscopy is suggested to be a quantitative descriptor of Li bond strength. These theoretical insights were further proved with actual cathode host materials and corresponding electrochemical tests. The development of Li bond theory and other theoretical scenarios will eventually propel the advancement in energy chemistry such as Li-S chemistry, Li metal chemistry, and redox flow chemistry through rational design and high throughput screening.

## Acknowledgements

This work was supported by National Key Research and Development Program (grant numbers 2016YFA0202500 and 2016YFA0200102), Natural Scientific Foundation of China (grant numbers 21676160 and 21561130151), and Tsinghua National Laboratory for Information Science and Technol-

ogy. We thank helpful discussion from Xi Zhang, Bo Li, Xin-Bing Cheng, Ze-Wen Zhang, Ge Zhang, Pei-Yan Zhai, and Jia-Le Shi.

### Conflict of interest

The authors declare no conflict of interest.

**Keywords:** ab initio calculations · electrochemistry · lithium bond · lithium–sulfur batteries · NMR spectroscopy

**How to cite:** *Angew. Chem. Int. Ed.* **2017**, *56*, 8178–8182  
*Angew. Chem.* **2017**, *129*, 8290–8294

- [1] N.-S. Choi, Z. Chen, S.-A. Freunberger, X. Ji, Y.-K. Sun, K. Amine, G. Yushin, L.-F. Nazar, J. Cho, P.-G. Bruce, *Angew. Chem. Int. Ed.* **2012**, *51*, 9994–10024; *Angew. Chem.* **2012**, *124*, 10134–10166; Y.-X. Yin, S. Xin, Y.-G. Guo, L.-J. Wan, *Angew. Chem. Int. Ed.* **2013**, *52*, 13186–13200; *Angew. Chem.* **2013**, *125*, 13426–13441.
- [2] A. Manthiram, Y. Fu, Y.-S. Su, *Acc. Chem. Res.* **2013**, *46*, 1125–1134.
- [3] P.-G. Bruce, S.-A. Freunberger, L.-J. Hardwick, J.-M. Tarascon, *Nat. Mater.* **2012**, *11*, 19–29; A. Rosenman, E. Markevich, G. Salitra, D. Aurbach, A. Garsuch, F.-F. Chesneau, *Adv. Energy Mater.* **2015**, *5*, 1500212; H.-J. Peng, X.-B. Cheng, J.-Q. Huang, Q. Zhang, *Adv. Energy Mater.* **2017**, *7*, 1700260; X. Liu, J.-Q. Huang, Q. Zhang, L.-Q. Mai, *Adv. Mater.* **2017**, *29*, 1601759; A. Manthiram, S.-H. Chung, C. Zu, *Adv. Mater.* **2015**, *27*, 1980–2006; Z.-W. Seh, Y.-M. Sun, Q.-F. Zhang, Y. Cui, *Chem. Soc. Rev.* **2016**, *45*, 5605–5634; J.-Q. Huang, Q. Zhang, F. Wei, *Energy Storage Mater.* **2015**, *1*, 127–145; J. Liang, Z.-H. Sun, F. Li, H.-M. Cheng, *Energy Storage Mater.* **2016**, *2*, 76–106.
- [4] X. Ji, S. Evers, R. Black, L.-F. Nazar, *Nat. Commun.* **2011**, *2*, 325.
- [5] N. Jayaprakash, J. Shen, S.-S. Moganty, A. Corona, L.-A. Archer, *Angew. Chem. Int. Ed.* **2011**, *50*, 5904–5908; *Angew. Chem.* **2011**, *123*, 6026–6030; Y.-S. Su, A. Manthiram, *Nat. Commun.* **2012**, *3*, 1166; H.-J. Peng, J. Liang, L. Zhu, J.-Q. Huang, X.-B. Cheng, X. Guo, W. Ding, W. Zhu, Q. Zhang, *ACS Nano* **2014**, *8*, 11280–11289; G. Zhou, S. Pei, L. Li, D.-W. Wang, S. Wang, K. Huang, L.-C. Yin, F. Li, H.-M. Cheng, *Adv. Mater.* **2014**, *26*, 625–631.
- [6] C. Tang, Q. Zhang, M.-Q. Zhao, J.-Q. Huang, X.-B. Cheng, G.-L. Tian, H.-J. Peng, F. Wei, *Adv. Mater.* **2014**, *26*, 6100–6105; L. Ma, H.-L. Zhuang, S.-Y. Wei, K.-E. Hendrickson, M.-S. Kim, G. Cohn, R.-G. Hennig, L.-A. Archer, *ACS Nano* **2016**, *10*, 1050–1059; L. Ma, H.-L. Zhuang, Y.-Y. Lu, S.-S. Moganty, R.-G. Hennig, L.-A. Archer, *Adv. Energy Mater.* **2014**, *4*, 1400390; J.-X. Song, T. Xu, M.-L. Gordin, P.-Y. Zhu, D.-P. Lv, Y.-B. Jiang, Y.-S. Chen, Y.-H. Duan, D.-H. Wang, *Adv. Funct. Mater.* **2014**, *24*, 1243–1250; J. Song, M.-L. Gordin, T. Xu, S. Chen, Z. Yu, H. Sohn, J. Lu, Y. Ren, Y. Duan, D. Wang, *Angew. Chem. Int. Ed.* **2015**, *54*, 4325–4329; *Angew. Chem.* **2015**, *127*, 4399–4403; B.-P. Vinayan, T. Diemant, X.-M. Lin, M.-A. Cambaz, U. Golla-Schindler, U. Kaiser, R. Jürgen-Behm, M. Fichtner, *Adv. Mater. Interfaces* **2016**, *3*, 1600372; Y.-L. Ding, P. Kopold, K. Hahn, P.-A. van Aken, J. Maier, Y. Yu, *Adv. Funct. Mater.* **2016**, *26*, 1112–1119.
- [7] T.-Z. Hou, H.-J. Peng, J.-Q. Huang, Q. Zhang, B. Li, *2D Mater.* **2015**, *2*, 014011.
- [8] T.-Z. Hou, X. Chen, H.-J. Peng, J.-Q. Huang, B.-Q. Li, Q. Zhang, B. Li, *Small* **2016**, *12*, 3283–3291.
- [9] Q. Zhang, Y. Wang, Z.-W. Seh, Z. Fu, R. Zhang, Y. Cui, *Nano Lett.* **2015**, *15*, 3780–3786; X.-Y. Tao, J.-G. Wang, C. Liu, H.-T. Wang, H.-B. Yao, G.-Y. Zheng, Z.-W. Seh, Q.-X. Cai, W.-Y. Li, G.-M. Zhou, *Nat. Commun.* **2016**, *7*, 11203; Z. Yuan, H.-J. Peng, T.-Z. Hou, J.-Q. Huang, C.-M. Chen, D.-W. Wang, X.-B. Cheng, F. Wei, Q. Zhang, *Nano Lett.* **2016**, *16*, 519–527; G. Zhou, H. Tian, Y. Jin, X. Tao, B. Liu, R. Zhang, Z.-W. Seh, D. Zhuo, Y. Liu, J. Sun, J. Zhao, C. Zu, D.-S. Wu, Q. Zhang, Y. Cui, *Proc. Natl. Acad. Sci. USA* **2017**, *114*, 840–845; X. Chen, H.-J. Peng, R. Zhang, T.-Z. Hou, J.-Q. Huang, B. Li, Q. Zhang, *ACS Energy Lett.* **2017**, *2*, 795–801.
- [10] L.-C. Yin, J. Liang, G.-M. Zhou, F. Li, R. Saito, H.-M. Cheng, *Nano Energy* **2016**, *25*, 203–210.
- [11] H.-J. Peng, G. Zhang, X. Chen, Z.-W. Zhang, W. T. Xu, J.-Q. Huang, Q. Zhang, *Angew. Chem. Int. Ed.* **2016**, *55*, 12990–12995; *Angew. Chem.* **2016**, *128*, 13184–13189.
- [12] K. Park, J. H. Cho, J.-H. Jang, B.-C. Yu, A.-T. De La Hoz, K.-M. Miller, C.-J. Ellison, J.-B. Goodenough, *Energy Environ. Sci.* **2015**, *8*, 2389–2395; K.-C. Kim, T. Liu, S.-W. Lee, S.-S. Jang, *J. Am. Chem. Soc.* **2016**, *138*, 2374–2382; K.-M. Liao, P. Mao, N. Li, M. Han, J. Yi, P. He, Y. Sun, H.-S. Zhou, *J. Mater. Chem. A* **2016**, *4*, 5406–5409.
- [13] D.-N. Shigorin, *Spectrochim. Acta* **1959**, *14*, 198–212.
- [14] A.-B. Sannigrahi, T. Kar, B.-G. Niyogi, P. Hobza, P.-V. Schleyer, *Chem. Rev.* **1990**, *90*, 1061–1076.
- [15] H.-J. Beister, S. Haag, R. Kniep, K. Strössner, K. Syassen, *Angew. Chem. Int. Ed. Engl.* **1988**, *27*, 1101–1103; *Angew. Chem.* **1988**, *100*, 1116–1118.
- [16] L. Pauling, *The nature of the chemical bond and the structure of molecules and crystals: An introduction to modern structural chemistry*, Vol. 18, Cornell University press, **1960**.
- [17] F. Cordier, M. Rogowski, S. Grzesiek, A. Bax, *J. Magn. Reson.* **1999**, *140*, 510–512.
- [18] R. Bhattacharyya, B. Key, H. Chen, A.-S. Best, A.-F. Hollenkamp, C.-P. Grey, *Nat. Mater.* **2010**, *9*, 504–510; N.-M. Trease, T.-K.-J. Köster, C.-P. Grey, *Electrochem. Soc. Interface* **2011**, *20*, 69–73; S. Chandrashekar, N.-M. Trease, H.-J. Chang, L.-S. Du, C.-P. Grey, A. Jerschow, *Nat. Mater.* **2012**, *11*, 311–315.
- [19] J. Xiao, J.-Z. Hu, H. Chen, M. Vijayakumar, J. Zheng, H. Pan, E.-D. Walter, M. Hu, X. Deng, J. Feng, B.-Y. Liaw, M. Gu, Z.-D. Deng, D. Lu, S. Xu, C. Wang, J. Liu, *Nano Lett.* **2015**, *15*, 3309–3316.
- [20] H.-J. Peng, T.-Z. Hou, Q. Zhang, J.-Q. Huang, X.-B. Cheng, M.-Q. Guo, Z. Yuan, L.-Y. He, F. Wei, *Adv. Mater. Interfaces* **2014**, *1*, 1400227; J. Zhang, H. Hu, Z. Li, X.-W. Lou, *Angew. Chem. Int. Ed.* **2016**, *55*, 3982–3986; *Angew. Chem.* **2016**, *128*, 4050–4054.

Manuscript received: April 26, 2017

Accepted manuscript online: May 18, 2017

Version of record online: June 9, 2017